JGR Oceans

RESEARCH ARTICLE
10.1029/2020JC016075

Pathways and Water Mass Transformation Along and Across the Mohn-Knipovich Ridge in the Nordic Seas

S. L. Ypma[1,2], S. Georgiou[1], J. S. Dugstad[3], J. D. Pietrzak[1], and C. A. Katsman[1]

[1]Department of Hydraulic Engineering, Civil Engineering and Geosciences, Environmental Fluid Mechanics, Delft University of Technology, Delft, Netherlands, [2]Institute for Marine and Atmospheric Research Utrecht, Utrecht University, Utrecht, Netherlands, [3]Geophysical Institute, Bjerknes Centre for Climate Research, University of Bergen, Bergen, Norway

Key Points:
- The northward flow along the Mohn Ridge does not form a one-to-one connection to the northward flow along the Knipovich Ridge
- Significant exchange takes place between the inner and outer branch of the Norwegian Atlantic Current north of 72° N
- Exchange across the mid-ocean ridge cools and freshens Atlantic Water as it travels north along the ridge

Correspondence to:
S. L. Ypma,
s.l.ypma@uu.nl

Citation:
Ypma, S. L., Georgiou, S., Dugstad, J. S., Pietrzak, J. D., & Katsman, C. A. (2020). Pathways and water mass transformation along and across the Mohn-Knipovich Ridge in the Nordic Seas. *Journal of Geophysical Research: Oceans*, *125*, e2020JC016075. https://doi.org/10.1029/2020JC016075

Received 12 JAN 2020
Accepted 30 JUL 2020
Accepted article online 3 AUG 2020

Abstract Atlantic Water takes various pathways through the Nordic Seas, and its transformation to denser waters forms a crucial connection to the lower limb of the Atlantic Meridional Overturning Circulation. Circulation maps often schematize two distinct pathways of Atlantic Water: one following the Norwegian Atlantic Slope Current along the continental slope of Norway and one following the Norwegian Atlantic Front Current along the Mohn and Knipovich Ridges. In this paper, the connectivity between the northward flow along these ridges is investigated. Analyzing trajectories of surface drifters and ARGO floats, we find that only 8% of the floats that travel near the mid-ocean ridges take the frontal pathway to the north. Indeed, by tracing numerical particles in a realistic numerical simulation, part of the water mass traveling along the Mohn Ridge follows the 2,500 m isobath eastward and joins the slope current, instead of flowing north along the Knipovich Ridge. Furthermore, north of 74°N, frequent exchange between the slope current and the front current is observed. Therefore, the slope current and front current are less isolated than often schematized. Additionally, the observational data set reveals substantial cross-ridge exchange; 31% of the floats that travel within 60 km from the mid-ocean ridges cross it. Results from numerical simulations indicate that the cross-ridge exchange leads to cooling and freshening of the Atlantic Water along the front. Deployments of floats near the mid-ocean ridges are needed to investigate the pathway of Atlantic Water and its exchange across the ridge in more detail.

Plain Language Summary The Atlantic Ocean plays a crucial role for global climate by redistributing heat and salt via the Atlantic Meridional Overturning Circulation (AMOC). A key region for maintaining this circulation is the Nordic Seas, where Atlantic Water is modified due to large ocean heat losses to the atmosphere. The transformation of Atlantic Water is not uniform, as the water mass can take various pathways. Two main routes are often described: one along the continental slope of Norway and one along the topographic ridges that separate the warm eastern basin from the cold western basin. In this paper, we investigate the latter pathway using a Lagrangian approach. That is, we follow the flow, instead of investigating properties at fixed positions. We find that the flow along the mid-ocean ridges is not continuous as often schematized; substantial exchange between the flow along the ridge and the flow along the continental slope occurs. Furthermore, we observe various trajectories that cross the mid-ocean ridge. Results from numerical simulations indicate that this cross-ridge exchange can lead to enhanced transformation of the Atlantic Water. Therefore, this process is important for setting the properties of water masses that enter the Arctic Ocean and of water masses that contribute to the AMOC.

1. Introduction

The Nordic Seas are characterized by a warm and saline Atlantic water mass in the east and a fresh and cold Arctic water mass in the west. Due to the anomalously warm and salty eastern basin, more than 60% of the total heat loss in the northern North Atlantic Ocean occurs in the Nordic Seas (Chafik & Rossby, 2019). As such, the transformed water masses leaving the Nordic Seas play a major role for the strength of the Meridional Overturning Circulation (MOC; e.g., Chafik & Rossby, 2019; Lozier et al., 2019). The upper limb of the MOC carries the warm Atlantic Water (AW) into the Nordic Seas via different branches (Figure 1a, Orvik & Niiler, 2002). The AW transforms to denser water masses along its path northward (e.g., Bosse et al., 2018), from where it flows toward the Arctic Ocean or returns south within the East Greenland Current (EGC). This gradual transformation of AW is seen as the main contributor to the

variability of the dense water leaving the Nordic Seas via the overflows (i.e., Eldevik et al., 2009; Mauritzen, 1996).

However, the AW in the eastern basin of the Nordic Seas cannot be seen as one homogeneous layer that is modified in a uniform way; upon entering the Nordic Seas, the AW follows various branches that affect different parts of the Nordic Seas (Hansen & Østerhus, 2000). AW circulation in the Nordic Seas is typically schematized by a two-branch structure (Orvik & Niiler, 2002). One branch, the Norwegian Atlantic Slope Current (NwASC, hereinafter the slope current), follows the Norwegian continental slope as a topographically controlled barotropic current. The second branch, the Norwegian Atlantic Front Current (NwAFC, hereinafter the front current), is a baroclinic jet associated with the Arctic Front (AF, Orvik & Niiler, 2002). The AF is characterized by a strong thermocline and halocline that separate the Arctic Water in the west from the AW in the east (Figure 1b Bosse & Fer, 2019). This density front is aligned with the mid-ocean topographic ridges in the Nordic Seas: the Mohn Ridge and the Knipovich Ridge (see Figure 1a). Along the Knipovich Ridge, the front current is often referred to as the western branch of the West Spitsbergen Current (Walczowski, 2013).

Hydrographic measurements at various sections across the AF reveal strong horizontal gradients in temperature and salinity along the topographic slope and show a clear northward flow along the ridges (i.e., Rossby, Ozhigin, et al., 2009; van Aken et al., 1995; Walczowski, 2013). Recent estimates from glider transects by Bosse and Fer (2019) indicate that the AW transport along the front current is comparable to the transport along the slope current (~3.2 Sv). It is therefore surprising that barely any surface drifters (Orvik & Niiler, 2002; Poulain et al., 1996) or RAFOS floats (Rossby, Prater, et al., 2009) follow this frontal pathway depicted in Figure 1a all the way through the Nordic Seas. The conclusion drawn by Orvik and Niiler (2002), that the NwAC maintains a two-branch structure throughout the Nordic Seas, was based on a composite of many partial pathways of surface drifters. Therefore, it can be questioned whether these pathways also apply to water parcels that come from south of 65°N and travel all the way to the Arctic. The fact that very few surface drifters follow the Mohn-Knipovich Ridge may be attributed to the nonuniform deployment and relatively large mortality of surface drifters in the Nordic Seas (Koszalka et al., 2011, 2013). But still, it is as of yet unclear whether the northward flow along the Mohn Ridge is connected to the downstream northward flow along the Knipovich Ridge in a Lagrangian sense.

Apart from AW modification in the along-front direction, across-front fluxes resulting from baroclinic instability of the front can impact water mass transformation processes. Evidence for such cross-frontal exchange is described by Budéus and Ronski (2009), who observed patches of AW in the Greenland Basin originating from the AF. In addition, analysis of satellite measurements and estimates from surface drifter data show enhanced eddy kinetic energy (EKE) along the Mohn Ridge (Koszalka et al., 2011; Trodahl & Isachsen, 2018). Analyses of hydrographic in situ measurements yield an eddy heat flux of 8–17.7 $\times 10^{12}$ W across the AF (van Aken et al., 1995; Walczowski, 2013). That is, ~30% of the total heat loss of the eastern basins in the Nordic Seas is due to eddy heat exchange with the colder and fresher western basins (Segtnan et al., 2011). The warm anticyclonic eddies shed by the front from east to west can be important for the deep convection processes in the Greenland Basin, as they provide a salt source that can sustain deep convection (Brakstad et al., 2019). In turn, the eddy-induced exchanges across the ridge cool and freshen the AW (Saloranta & Svendsen, 2001), which affects the overturning in the Nordic Seas and the properties of the water masses entering the Arctic.

However, no significant cross-ridge exchange is captured by trajectories of surface drifters (Poulain et al., 1996), subsurface RAFOS floats (Rossby, Prater, et al., 2009), or ARGO floats (Latarius & Quadfasel, 2016; Voet et al., 2010). In fact, Rossby, Ozhigin, et al. (2009) suggest that cross-ridge exchange is unlikely, as the AF density gradient is strong and tightly locked to the sloping topography. Furthermore, analyses of a SF6 tracer, injected in the Greenland basin in 1996, do not show significant mixing between the Greenland Basin and the Lofoten Basin (Messias et al., 2008; Olsson et al., 2005). It is therefore unclear how important the cross-front transport is for water mass transformations in the Nordic Seas.

Successive analyses of the growing Lagrangian observational data set have shown to continuously improve understanding of the Nordic Seas surface and mid-depth circulation and variability (Dugstad, Fer, et al., 2019; Koszalka et al., 2011; Poulain et al., 1996; Rossby, Prater, et al., 2009; Orvik & Niiler, 2002; Voet et al., 2010). Therefore, in this paper we revisit the surface drifter and ARGO float trajectories with a special focus

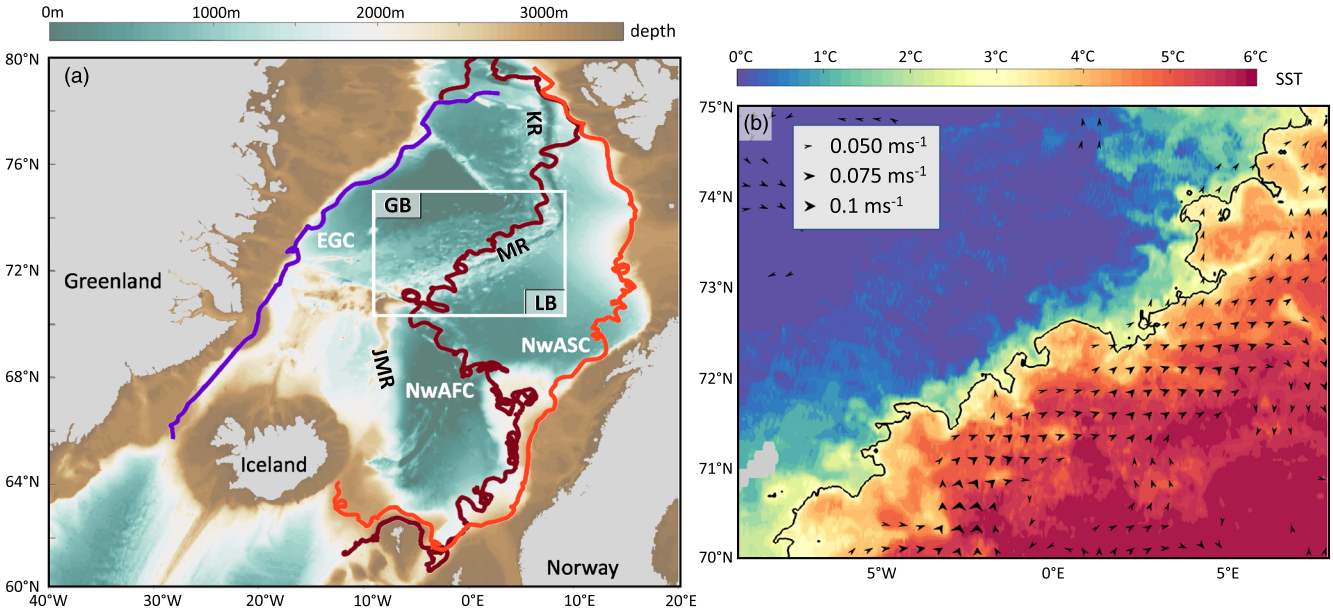

Figure 1. (a) Bathymetry of the Nordic Seas and pathways of three example surface drifters that follow the Norwegian Atlantic Slope Current (NwASC, orange path), the Norwegian Atlantic Front Current (NwAFC, dark red path), and the East Greenland Current (EGC, blue path). The bathymetric features pertinent for this study are marked: the Mohn Ridge (MR), the Knipovich Ridge (KR), and the Jan Mayen Ridge (JMR). Bathymetry is from ETOPO1 (Smith & Sandwell, 1997). (b) Sea surface temperature (SST) from AVHHR sensor at the location of the white box indicated in the left panel; image on 29 April 2017, showing the Arctic Front (3°C contour is highlighted). The black arrows show the mean geostrophic velocity from AVISO satellite altimetry for the year 2017 for velocities stronger than 0.04 m s^{-1}.

on trajectories along and across the Mohn and Knipovich Ridges. In order to investigate the connection between the flow along the Mohn and Knipovich Ridges and possible pathways across the ridges, results from the observed trajectories are compared to trajectories from a realistic, high-resolution numerical calculation (section 3). Furthermore, the importance of baroclinic cross-ridge exchange for water mass transformation along AW pathways is investigated in an idealized numerical configuration of the Lofoten and Greenland Basins as well (section 4). A discussion and conclusions are provided in section 5.

2. Methods

When investigating pathways and connectivity between different ocean branches, a Lagrangian approach is most suitable (Bower et al., 2019; van Sebille et al., 2018). Therefore, we use all trajectories available from surface drifters and ARGO floats that at some moment during their lifetime passed through the Nordic Seas. Details on this data set and the selection procedure to analyze the flow along and across the Mohn and Knipovich Ridges are provided in section 2.1. The observed trajectories are limited not only in quantity but also in their capability to trace water masses. As ARGO floats and surface drifters float at a fixed depth, they are unable to represent any vertical displacement of water masses, which is likely to occur in the Nordic Seas. Therefore, we performed additional Lagrangian studies to evaluate pathways and water mass transformation of AW along the mid-ocean ridges using both a high-resolution, realistic ocean model (section 2.2) and an idealized numerical simulation (section 2.3).

2.1. Trajectories From Observations

The surface drifter data set is obtained from the Global Drifter Program (GDP) database (https://www.aoml.noaa.gov/phod/gdp/ updated through 30 June 2019 when downloaded on 3 December 2019). The surface drifters consist of a buoy at the surface and a subsurface drogue, and their trajectories represent the circulation at 15 m depth. Trajectories of surface drifters that have lost their drogue are not taken into account. A quality control and interpolation of each drifter position to 6 hr intervals were performed by the AOML/NOAA Drifter Data Assembly Center (Lumpkin & Pazos, 2007).

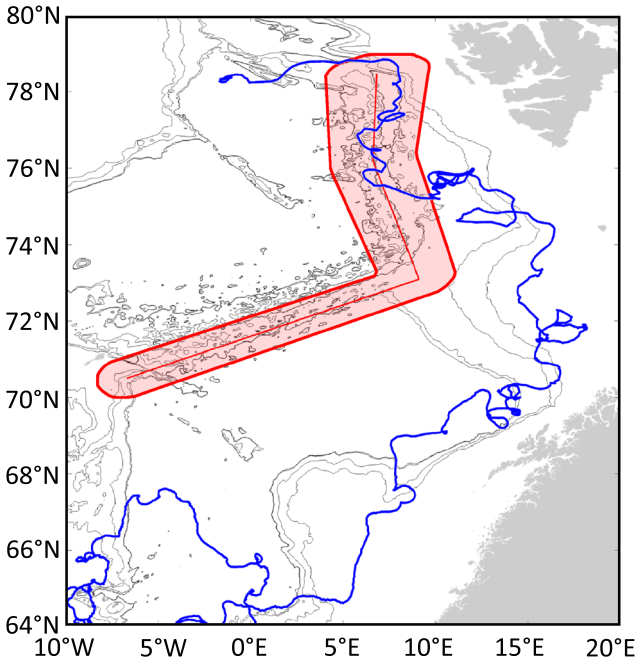

Figure 2. Selection area (red shading) for floats traveling close to the Mohn and Knipovich Ridges. The red straight line follows the 2,250 m isobath along the Mohn and Knipovich Ridges, and red shading indicates the 60 km radius from this line. The blue line shows an example path of a surface drifter following part of the Knipovich Ridge. The 1,000, 1,500, 2,000, and 2,500 m isobaths are shown in gray.

In contrast to surface drifters, ARGO floats typically drift at 1,000 m depth. Every 10 days, they descend to 2,000 m depth and subsequently ascend to the surface profiling the water column. At the surface, they transmit their data and position to a satellite and return to their parking depth. Tracing the profiling location of ARGO floats visualizes the circulation at mid-depth (Voet et al., 2010). The ARGO float data are obtained from the International Argo Program (downloaded on 18 November 2019 from https://coriolis.eu.org), and only quality-controlled profiles are taken into account.

At time of download (3 December 2019), 564 surface drifters and 283 ARGO floats had been drifting through the Nordic Seas. To investigate the flow along and across the Mohn and Knipovich Ridges, trajectories that came in close vicinity to the mid-ocean ridges are selected. To this end, it is assumed that the front current flows along the 2,250 m isobath (Bosse & Fer, 2019), which is schematized by a straight line in Figure 2. The width of the front is estimated to be ~40 km (Bosse & Fer, 2019), but the position of the front itself can be variable. Therefore, an area is defined by a 60 km radius from the 2,250 m isobath (red shading in Figure 2). Every float or drifter entering this area is used for analysis. This way, only 40 surface drifters and 50 ARGO floats remain, which allows for subsequent separation based on individual pathways by eye.

2.2. Trajectories From a Realistic Ocean Model

As the number of surface drifters and ARGO floats in the vicinity of the mid-ocean ridges is relatively low, results from the observed trajectories are compared to trajectories from a realistic ocean model: the Regional Ocean Modeling System (ROMS) applied to the eastern Nordic Seas (Figure 3a). The model has 800 m horizontal resolution and 60 vertical levels, ranging from 2–5 m at the surface to 60–70 m near the bottom. Details on the model configuration can be found in Dugstad, Koszalka, et al. (2019). Thanks to its high spatial resolution, the model resolves mesoscale and some of the submesoscale processes in the Nordic Seas and captures the variability and dynamics of the area well (Dugstad, Koszalka, et al., 2019; Trodahl & Isachsen, 2018).

We use the Lagrangian data set obtained by Dugstad, Koszalka, et al. (2019), who created this data set to investigate variability of the inflow to the Lofoten Basin. They used the 6-hourly output of the 3-D velocity fields from the realistic model, spanning years 1996 to 1999, to advect numerical particles. These particles were deployed in a rectangular grid of 40×40 drifters (white dots, Figure 3a) every week for 3 years at three different depth levels (15, 200, and 500 m). This spatially uniform deployment allows for a better representation of the flow, in contrast to the observed drifters and floats that are deployed along specific sections and in locations, which can lead to limited and biased statistics (Dagestad et al., 2018). The particles were advected for 1 year using the OpenDrift tool with a fourth-order Runga Kutta time stepping scheme (Dagestad et al., 2018, OpenDrift is an open source code that can be accessed at https://github.com/OpenDrift/opendrift). No explicit horizontal or vertical diffusion was added. Dugstad, Koszalka, et al. (2019) showed that turbulent transport processes are well captured by this data set.

Here, the data set is analyzed to study the pathways of AW along the mid-ocean ridge to the north. As we are only interested in AW, deployments northwest of the Mohn Ridge are not taken into account. Moreover, only particles that leave the domain within the advection time and were deployed at 200 m depth are considered. In this way, 115,515 trajectories are selected. The mean northward velocity is used to separate the trajectories further based on where the particles leave the domain (see solid red lines in Figure 3b). Particles that flow along the continental slope of Norway leave the domain between 9.5°E and 16.4°E; particles that follow the Knipovich Ridge leave the domain between 2.5°E and 9.5°E.

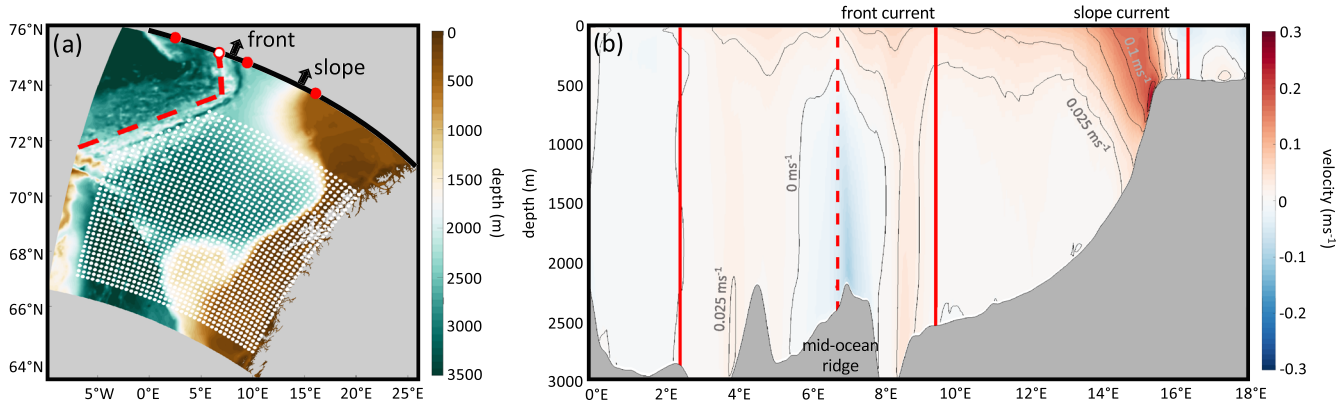

Figure 3. (a) Bathymetry of the realistic numerical simulation described in section 2.2. White dots indicate the deployment locations of particles at 200 m depth. The red dots correspond to the transects shown in panel (b). (b) Cross section of the mean meridional velocity at the northern boundary of the model domain (red shading indicates northward flow). Red solid lines indicate the transects used to separate particles that leave the domain via the slope current from those that leave via the front current. The red dashed lines in panels (a) and (b) show the transect used to separate the particles that follow the mid-ocean ridge from the particles that enter the Greenland Basin as described in section 4.

2.3. Trajectories From an Idealized Numerical Configuration

As the realistic ocean model simulates only part of the eastern Nordic Seas, an idealized configuration of the Massachusetts Institute of Technology general circulation model (MITgcm, Marshall et al., 1997) is used to shed light on the connection between the eastern (Lofoten) and western (Greenland) basin. Furthermore, the importance of the frontal instability for AW transformation is investigated using this model. Although

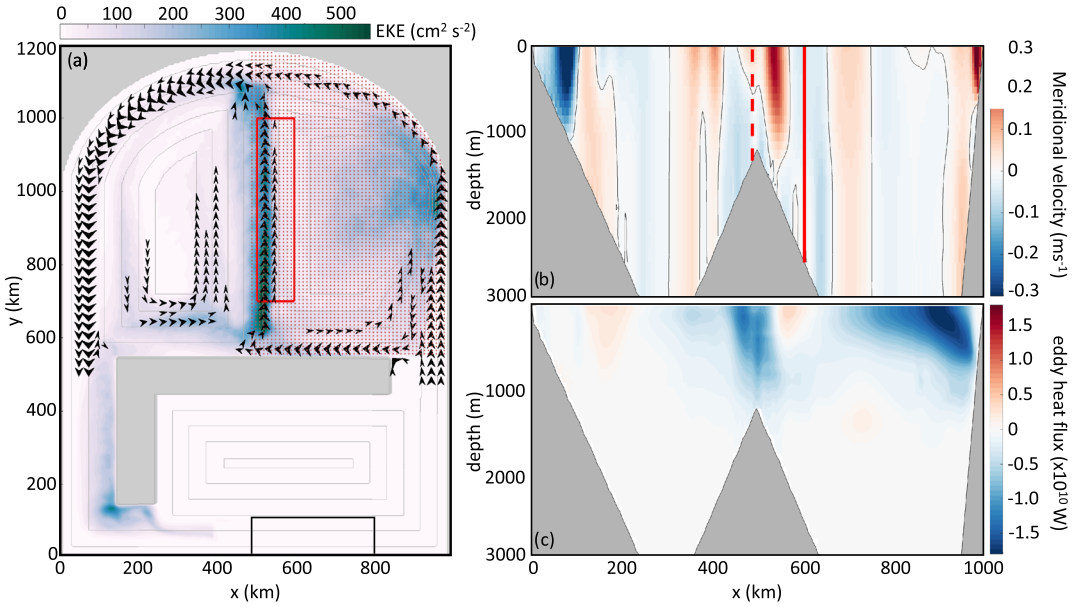

Figure 4. (a) Five-year mean surface eddy kinetic energy (blue shading) and surface velocity >0.05 m s^{-1} north of the sill (black arrowheads) in the idealized numerical simulation. Gray contours depict the model bathymetry (contour interval is 500 m). The black box south of the island indicates the region where the model temperature and velocity are restored. Particles are released at 200 m depth on a 15 km × 15 km grid east of the ridge and north of the island (red dots). Only particles that enter the region indicated by the red box are used for the analysis. (b) Cross section at $y = 750$ km of the 5 year mean meridional velocity (shading), the zero velocity contour is shown in gray. The red lines correspond to the zonal extent of the box shown in panel (a). The red dashed line is used to separate the particles that follow the mid-ocean ridge from the particles that enter the western basin as described in section 4. (c) Zonal eddy heat flux as a function of depth, integrated over the full meridional extent of the domain north of the island.

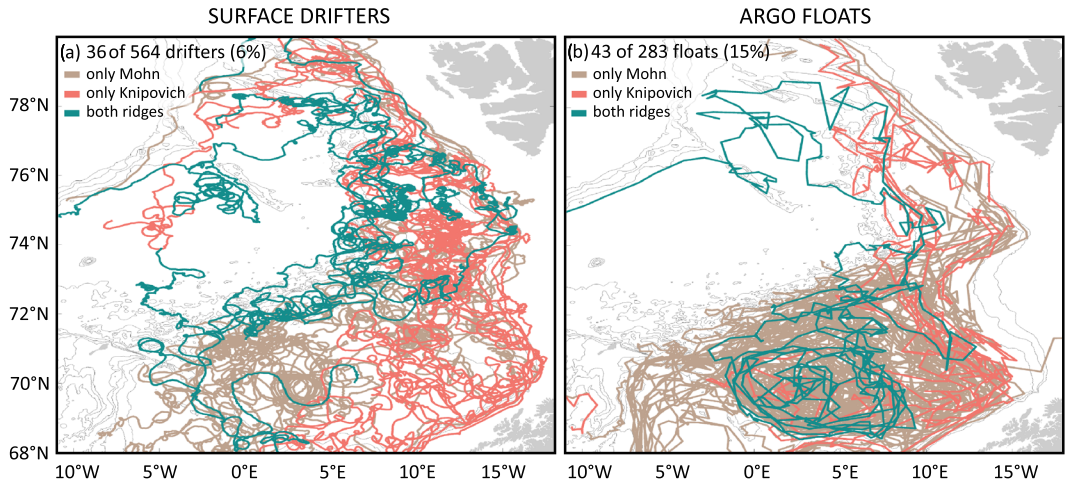

Figure 5. Trajectories of all (a) surface drifters and (b) ARGO floats that flow along part of the Mohn Ridge (brown lines), the Knipovich Ridges (orange lines), or both ridges (green lines). The 1,000, 1,500, 2,000, and 2,500 m isobaths are shown in gray. The percentage given in each panel indicates how many surface drifters or ARGO floats travel close to the mid-ocean ridges compared to the total number of available surface drifters and ARGO floats, respectively.

idealized, the model captures the dynamics of the Nordic Seas pertinent for this study (Ypma et al., 2020). The model has a 5 km horizontal resolution and 33 vertical levels ranging from 20 m thickness at the surface to 200 m thickness near the bottom. The warm eastern basin is separated from a colder western basin by a mid-ocean ridge at 1,200 m depth (Figure 4). Details on the model configuration, as well as on the hydrodynamic properties of the circulation, can be found in Spall (2011) and Ypma et al. (2020).

The model domain consists of two parts separated by an island. The area north of the island represents the Lofoten and Greenland Basins. There, the ocean surface temperature is restored to an atmospheric temperature of 4°C with a timescale of 2 months to resemble a realistic surface heat flux (Ypma et al., 2020). Furthermore, temperature and velocity are restored over the full water column south of the island (see black box Figure 4a); no other surface forcing is applied. This induces a buoyant cyclonic boundary current, representative of the AW inflow. This inflow separates into a slope current and a front current, mimicking the NwASC and NwAFC, respectively (arrowheads in Figure 4a). As described in, for example, Spall (2010) and Isachsen (2015), the steepening of the continental slope near the Lofoten Islands is essential to create the observed enhanced eddy activity that induces the advection of AW throughout the eastern basins of the Nordic Seas. The idealized model captures the magnitude of EKE near the steep slope (shading in Figure 4a). Enhanced eddy variability is also found along the unstable front current. The total eddy heat flux across the thermal front in the idealized model is 10×10^{12} W (Figure 4c), which is of similar magnitude as estimated from observations by van Aken et al. (1995) and Walczowski (2013).

To investigate the water mass transformation of the AW in this model, numerical particles are released every 15 km × 15 km east of the ridge at 200 m depth similar to the approach in the realistic numerical simulation (red dots in Figure 4a). The particles are advected forward in time along their 3-D trajectories using the Connectivity Modeling System (CMS, Paris et al., 2013) within the daily averaged three-dimensional velocity fields of the MITgcm simulation. A time step of 1 hr is used, and the new position of each particle is calculated using a fourth-order Runge Kutta stepping scheme in time and a tricubic interpolation in space. As for the realistic simulation, no horizontal or vertical diffusivity is added to the particles, so the particle motion is purely advective.

Particles are released daily for only 30 days and advected for 4 years. This is sufficient to capture the variability of the eastern basin since the idealized model simulation does not have a seasonal cycle. As we are interested in the dynamics of the front current, only those particles that have traveled within part of the front current are selected (red box Figure 4a and red lines Figure 4b). This results in 59,346 particles that are used for the analysis.

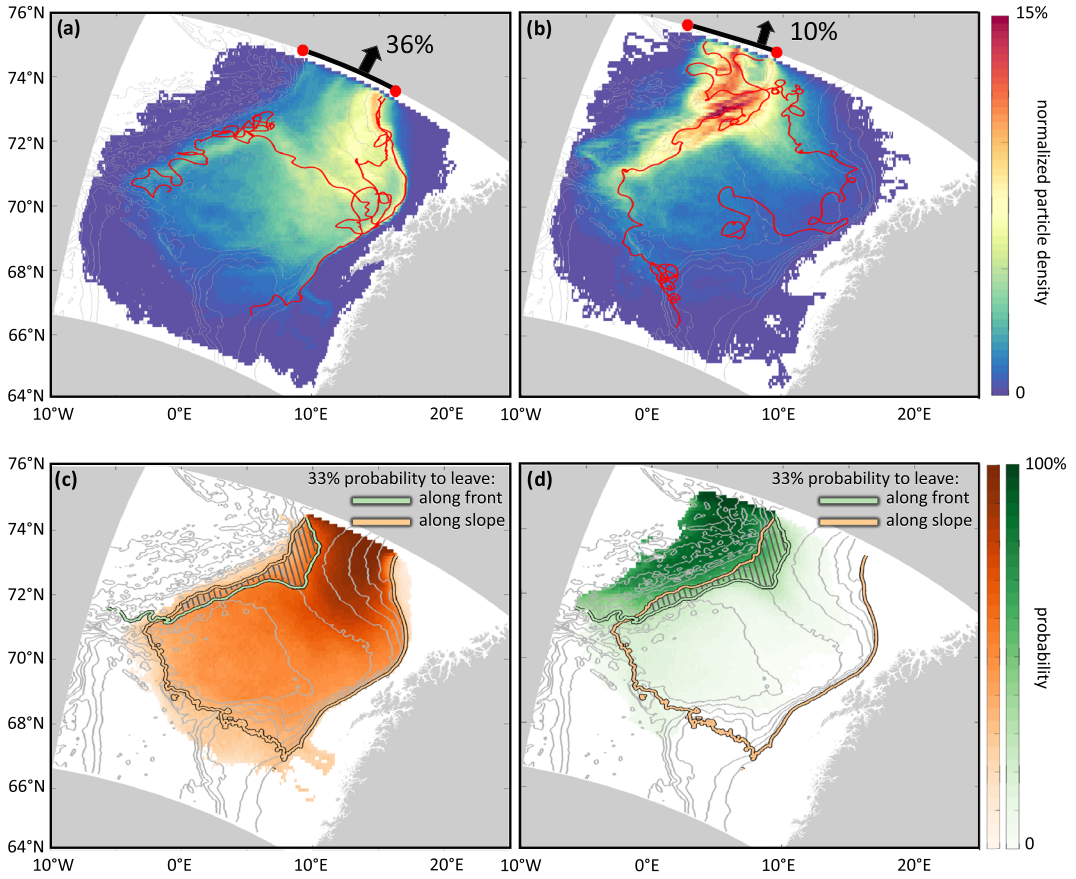

Figure 6. Normalized particle density map of particles deployed at 200 m that (a) leave the model domain along the continental slope or (b) leave along the Knipovich Ridge. Each particle position is regridded on a 0.1° lon × 0.1° lat grid. Example trajectories of each pathway are indicated by the red lines. Isobaths are shown in gray (500 m contour interval). (c, d) The probability that a particle will leave the domain along (c) the slope or (d) the mid-ocean ridge is given by the number of particles that cross each 0.1° lon × 0.1° lat gridbox and leave through the specified transect divided by the total number of particles that cross that gridbox. The 33% probability contours are indicated by the orange (particles that leave along the slope) and green line (particles that leave along the front). Results shown are diagnosed from the realistic numerical simulation (section 2.2).

3. Along and Across Frontal Pathways

In this section, the connection between the frontal currents along the Mohn and Knipovich Ridges is investigated using both the trajectories from surface drifters and ARGO floats (as described in section 2.1) and the trajectories from the realistic numerical simulation (as described in section 2.2). Furthermore, pathways that reveal cross-ridge exchange between the Lofoten Basin and the Greenland Basin are discussed.

Most of the pathways taken by the surface drifters that come near the ridge (red shaded area in Figure 2) follow only part of the mid-ocean ridges as highlighted by the pathways in Figure 5a. From the 36 surface drifters that travel along the mid-ocean ridges, only five follow the path northward along both the Mohn Ridge and the Knipovich Ridge (green trajectories in Figure 5a). All other trajectories display a path that alternates between the slope current and the front current as indicated by the orange and brown trajectories in Figure 5a. Most surface drifters that flow along the Mohn Ridge (brown trajectories, 9 of the 17 floats) are steered eastward by the 2,500 m isobath at 72°N and continue their journey as part of the slope current. Most surface drifters that flow along the Knipovich Ridge (orange trajectories, 8 of the 14 floats) originate from the slope current. North of 74°N, many drifter pathways show exchanges between the western and eastern branch of the West Spitsbergen Current. Numerous surface drifter paths display loops, indicative of mesoscale eddies.

This exchange between the slope and front currents north of 72°N is also displayed by the trajectories of the ARGO floats (Figure 5b). In total, 10 of the 43 floats flow along the Knipovich Ridge and originate from the slope current. The mean flow at 1,000 m depth along the Mohn Ridge is southward (Voet et al., 2010). So most of the floats that follow the Mohn Ridge travel south (39 of 43 floats) and leave the Lofoten Basin along the Jan Mayen Ridge (27 of 43 floats). Furthermore, as most of the ARGO floats were originally deployed in the basin interior, the floats tend to follow the closed cyclonic circulation within the Lofoten Basin (Voet et al., 2010). It is therefore not surprising that only two ARGO floats show a connection between the northward flow along the Mohn Ridge and the Knipovich Ridge.

As the number of surface drifters and ARGO floats that approach the mid-ocean ridges is limited, trajectories in the realistic model configuration released at 200 m depth (section 2.2) are used to investigate the connection between the slope and front currents in more detail. The numerical particles that leave the model domain toward the north(west) are separated in two pathways: one along the continental slope (36% of the total number of particles; Figure 6a) and one along the Knipovich Ridge (10% of the total number of particles; Figure 6b). Most of the other particles leave the domain toward the southeast along the Jan Mayen Ridge or to the north within the Norwegian Coastal Current (54%).

The normalized particle density distribution in Figure 6 highlights which pathways the numerical particles take depending on where they leave the domain. Just as observed in the trajectories of the surface drifters, some of the trajectories along the Mohn Ridge follow the 2,500 m isobath at 72°N toward the southeast to join the slope current. Vice versa, some of the trajectories that follow the slope current flow along the same isobath toward the northwest to join the flow along the Knipovich Ridge (see example trajectories in Figures 6a and 6b). Therefore, the trajectories in the realistic numerical simulation, in line with the observed trajectories (Figure 5), suggest substantial exchange between the front current and the slope current, before these branches continue north of 72°N.

The connection between the front and the slope currents is further investigated by computing the probability that a particle at any given location will leave the domain via the continental slope or via the Knipovich Ridge (Figures 6c and 6d). The probability is given by the ratio of the number of particles that cross a gridbox and leave the domain at a specified location to the number of particles that cross that gridbox in total. Therefore, darker shading in Figures 6c and 6d indicates a large probability that a particle in that region will leave via the continental slope (Figure 6c) or via the Knipovich Ridge (Figure 6d).

Along the entire length of the Mohn Ridge, particles display a similar probability (>33%) of leaving the domain via the slope current and leaving the domain along the Knipovich Ridge (striped area in Figures 6c and 6d). This again emphasizes the exchange between the front and slope currents and reveals that the flow along the Mohn Ridge does not form a one-to-one connection with the flow along the Knipovich Ridge.

An interesting aspect of the pathway highlighted by the particle density distribution in Figure 6b is that some particles shift from the eastern flank of the Mohn Ridge to the western flank of the Knipovich Ridge. Furthermore, ∼2% of the total outflow in the realistic numerical simulation consists of particles that cross the mid-ocean ridge from the Lofoten Basin into the Greenland Basin (not shown). The individual trajectories show strong variability along and northwest of the Mohn Ridge. As they originate from the AW layer in the east, they could represent AW from the frontal current detached by frontal instabilities traveling into the Greenland Basin as observed by Budéus and Ronski (2009).

The observed trajectories of surface drifters reveal the instability of the front current as well (Figure 7a). Especially along the Knipovich Ridge, multiple surface drifters cross the summit of the ridge and show meandering or circular (eddying) trajectories near the ridge. The trajectories of the 14 surface drifters shown in Figure 7a all indicate significant cross-ridge exchange between the Lofoten and the Greenland Basins.

Furthermore, 14 ARGO floats are found to cross the mid-ocean ridge from the Greenland Basin into the Lofoten Basin (or vice versa; Figure 7b). However, the cross-ridge exchange at the ARGO float depth is not necessarily related to the frontal instability. A zoom-in of four ARGO float trajectories near the ridge is shown in Figure 8. Three of these floats start in the cyclonic gyre of the Greenland Basin (Figures 8a–8c). When they approach the ridge, they cross, travel southward, and start to follow a

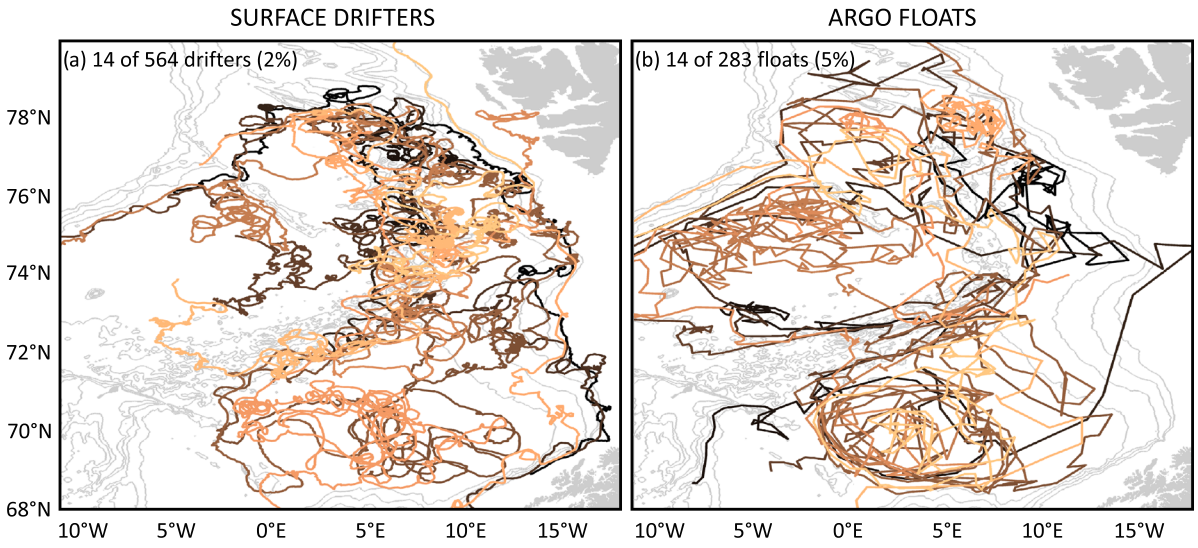

Figure 7. Pathways of (a) drifters and (b) ARGO floats that cross the Mohn and Knipovich Ridges (coloring is random). The 1,000, 1,500, 2,000, and 2,500 m isobaths are shown in gray. The percentage given in each panel indicates how many drifters or floats crossed the ridge compared to the total number of available surface drifters and ARGO floats, respectively.

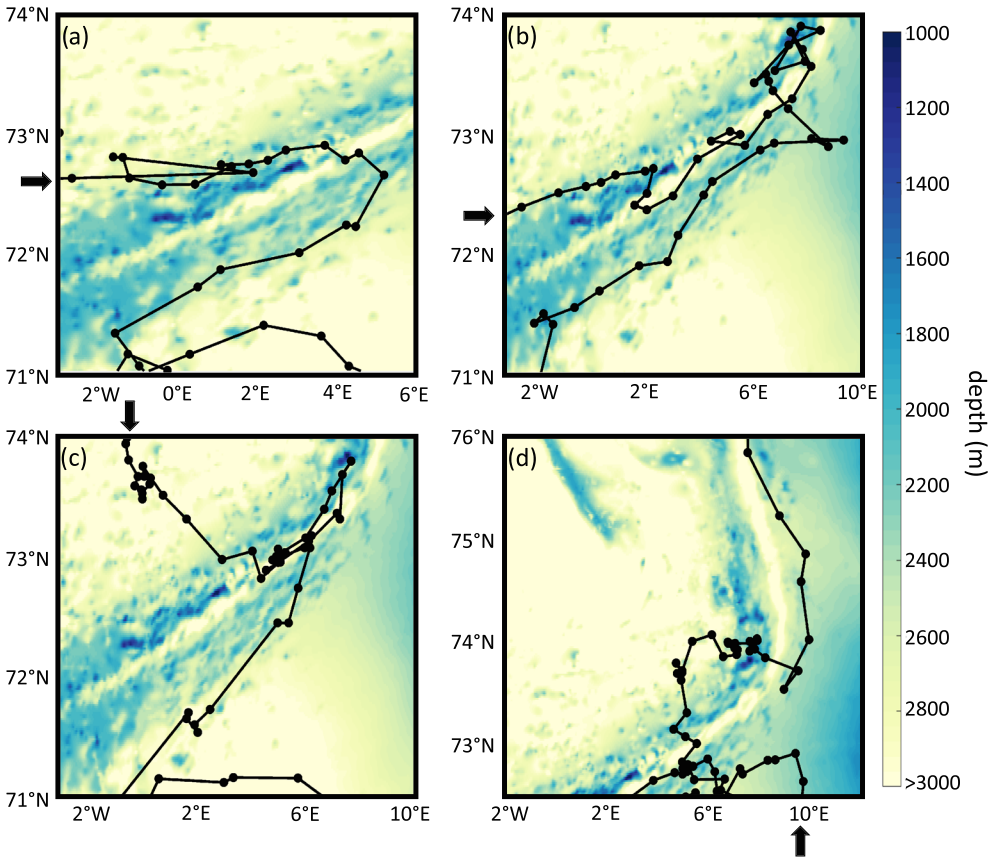

Figure 8. Four examples of ARGO float trajectories that cross (a–c) the Mohn Ridge and (d) the Knipovich Ridge (black lines). The arrows indicate the travel direction of the floats, and shading shows the bathymetry from ETOPO1 (Smith & Sandwell, 1997).

cyclonic circulation along the outer rim of the Lofoten Basin. The example trajectory in Figure 8d shows similar behavior, except that the float continues its path northward along the Knipovich Ridge.

It is beyond the scope of this study to assess the mechanisms behind the cross-ridge behavior of the ARGO floats. The position of the ARGO floats is only known at specific moments in time and the bathymetry near the mid-ocean ridges in the Nordic Seas is very complex. However, exchange between the western and eastern basins through gaps in the topographic ridges has been hypothesized by e.g., Spall (2010). Although Olsson et al. (2005) and Messias et al. (2008) showed that a fast pathway to exit the Greenland Basin exists via the Jan Mayen Current, the ARGO floats shown here that originate from the Greenland Basin do not seem to have a preferred location where they cross the mid-ocean ridge. Not surprising, they seem to be steered much stronger by topography than the surface drifters that showed cross-ridge exchange. Possibly, enhanced mean flow within canyons as discussed by Ruan and Callies (2019) can lead to the behavior seen by the ARGO floats.

In conclusion, results from surface drifter trajectories (Figure 5a), ARGO float trajectories at 1,000 m (Figure 5b) and trajectories in a realistic numerical configuration at mid-depth (Figure 6) all indicate that the connection between the flow along the Mohn Ridge and the flow along the Knipovich Ridge is not as strong as suggested by surface circulation schematics currently in use (e.g., Orvik & Niiler, 2002). Furthermore, several surface drifters and ARGO floats cross the mid-ocean ridge from one basin into the other. Therefore, in addition to the large eddy variability in the Lofoten Basin (Bosse et al., 2018), the enhanced exchange between the slope current and the front current north of 72°N and the excursions of water masses across the mid-ocean ridge lengthen the residence time of the AW within the eastern basin of the Nordic Seas. This potentially has implications for the water mass transformation of the AW in the eastern basin, which is discussed in the following section.

4. Importance of Frontal Instability for Water Mass Transformation

Next, we investigate the dependence of AW transformation on possible pathways related to the instability of the front current. The realistic numerical configuration is limited by its domain, and the low number of ARGO floats and surface drifters available near the front current is not sufficient to perform any statistical analysis on water mass transformation. Furthermore, since the surface drifters and ARGO floats drift at a specified pressure level, they are not suited to trace a particular water mass that might move in the vertical. Therefore, the fate of the AW is also traced in the idealized model configuration of the Lofoten and Greenland Basin introduced in section 2.3. In this section, the frontal pathways and AW transformation found in the idealized model configuration are compared to the results from the realistic numerical configuration.

To investigate the role of the frontal instability, only those particles are taken into account that leave the domain within the front current (realistic numerical configuration; see section 2.2) or traveled within the front current (idealized numerical configuration; see section 2.3). Furthermore, particles that follow the mean flow along the mid-ocean ridge are separated from the particles that at some point along their trajectory meander into the Greenland (western) Basin. In both model simulations, the mean flow along the mid-ocean ridge is mainly confined to a constant isobath (dashed red lines in Figures 3a, 3b, 4a, and 4b). Particles that do not cross this isobath are assumed to follow the front current to the north (*front*-pathway); particles that do cross this isobath are assumed to be steered into the western basin by the instability of the front current (*front_west*-pathway).

By applying this selection procedure to the particles in the realistic model, the two exit pathways along the eastern and western flank of the Knipovich Ridge that were already identified in Figure 6b are now separated (Figures 9a and 9b). The *front*-pathway consists of particles that partly follow the Mohn Ridge but also originate from the slope current. In contrast, the *front_west*-pathway mainly consists of particles that travel along the Mohn Ridge. Most of these particles cross the mid-ocean ridge toward the northwest at 73°N where they continue their path along the western flank of the Knipovich Ridge.

The particles in the idealized numerical simulation display a similar behavior (Figures 9c and 9d). The *front*-particles indicate exchange with the slope current mainly in the northern part of the domain, whereas the *front_west*-particles reside mainly at the western side of the front current. Therefore, the *front_west*-

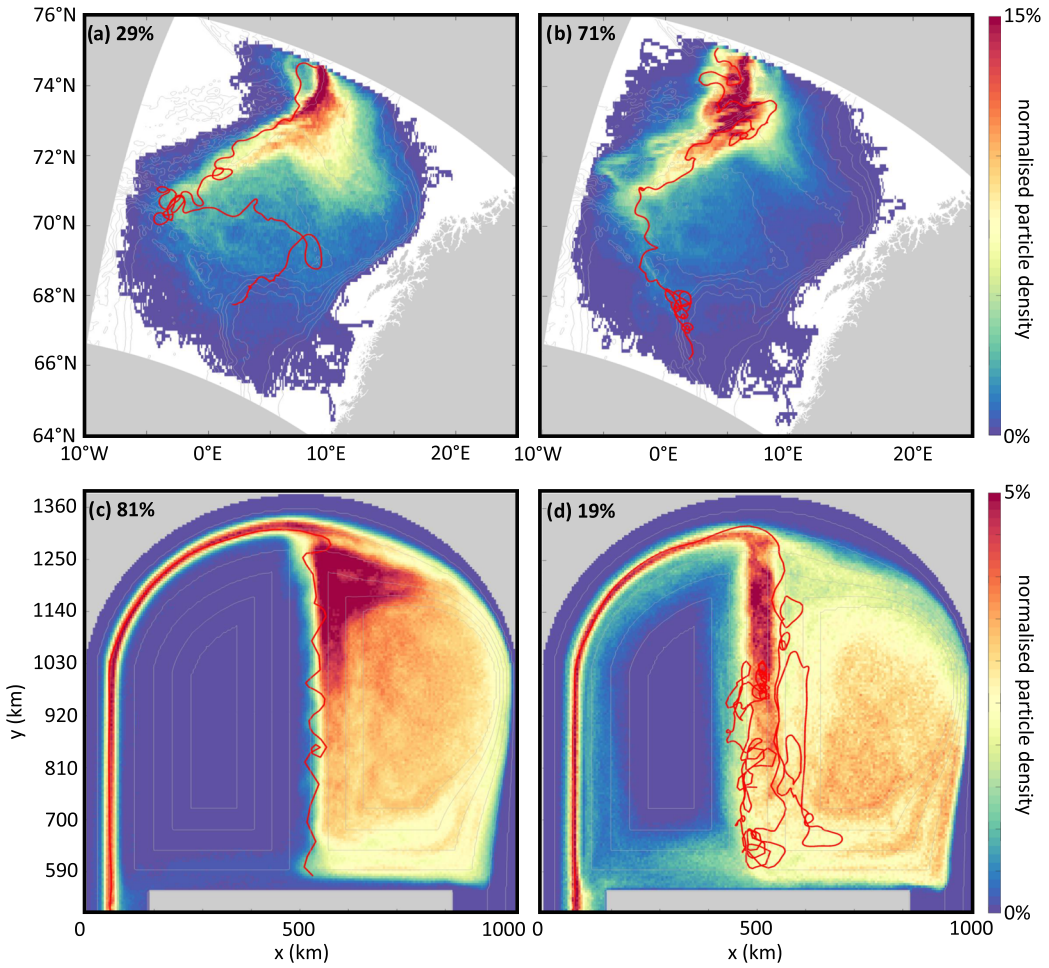

Figure 9. Normalized particle density map of the (a, c) *front*-pathway and the (b, d) *front_west*-pathway in the (a, b) realistic and (c, d) idealized model simulation. Each particle position is regridded on a 11 × 11 km *x*-*y* grid (0.1 × 0.1° lon × lat grid) in the idealized (realistic) simulation. Example trajectories of each pathway are indicated by the red lines. Gray lines show isobaths. The percentage given in each panel indicates how many particles follow the *front*-pathway or the *front_west*-pathway compared to the total number of particles that follow the mid-ocean ridges in the models.

particles are found farther offshore within the boundary current in the western basin compared to the *front*-particles. Unlike the particles in the realistic simulation, there is no strong evidence for a preferred location where the *front_west*-particles cross the ridge into the western basin. This can be explained by the uniform shape of the mid-ocean ridge in the idealized numerical configuration.

Despite the similarities of the frontal pathways in the realistic and the idealized simulations, the number of particles that follow the *front*-pathway and *front_west*-pathway differ between the two simulations. In the realistic simulation, most particles (71%) cross the ridge and flow along the western flank of the Knipovich Ridge, whereas in the idealized simulation, most particles (81%) stay within the mean flow of the front current. Note that the percentages calculated are based on the total number of particles following each path, not on the total transport carried. Furthermore, although the idealized numerical configuration captures some of the key features of the Nordic Seas, a realistic bathymetry and surface forcing (e.g., there is no wind forcing in the idealized configuration) will certainly play a role on the strength and separation of various pathways within the Nordic Seas. However, as the frontal instability is mostly a result of the strong horizontal gradients in density across the ridge, the idealized configuration can still be used to investigate water mass transformation processes occurring along the front.

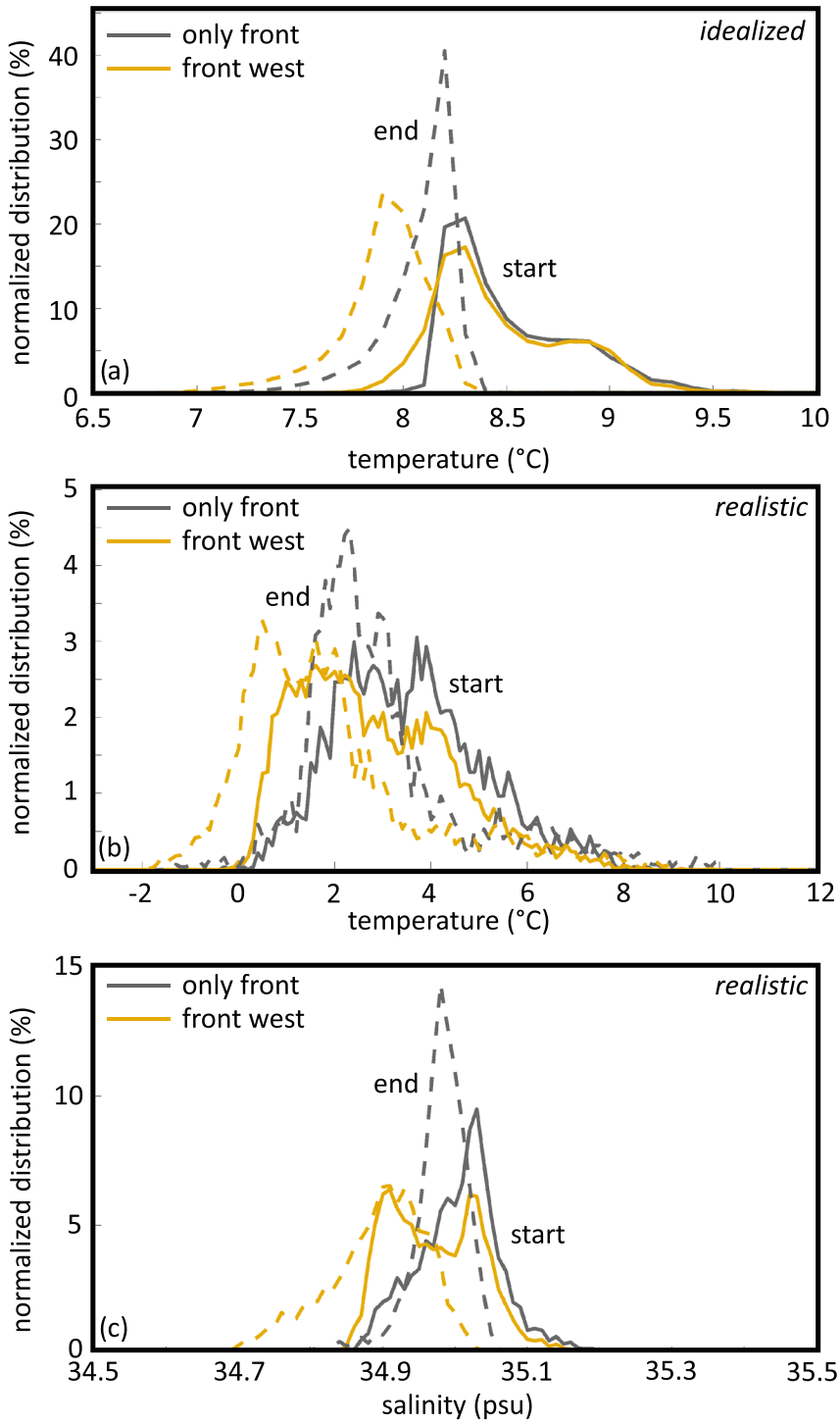

Figure 10. (a, b) Temperature and (c) salinity distribution of particles that leave the domain taking the *front*-pathway (gray lines) or the *front_west*-pathway (yellow lines) at the start of deployment (solid lines) and when leaving the domain (dashed lines). Results shown are diagnosed from the (a) idealized and (b, c) realistic numerical simulation. A binsize of 0.1°C and 0.01 psu for temperature and salinity are used, respectively. Note that different limits for temperature are used in panels (a) and (b) and that density in the idealized simulation depends on temperature only.

To assess the impact of the frontal current instability on the water mass transformation in the idealized basin, for each pathway the temperature of the particles at the deployment location is compared to the temperature at the outflow (Figure 10a). The distribution of the particles' temperature at the outflow shows two distinct peaks at ~8.2° C and ~7.9° C (dashed lines Figure 10a). The colder signal at the outflow is related to the pathways that interact with the western basin interior (the *front_west*-particles; yellow lines in Figure 10a), whereas the warmer outflow waters correspond to the particles that travel within the front (the *front*-pathway; gray lines). Note that the temperature distribution of the *front*-particles and *front_west*-particles is indistinguishable at deployment (solid gray and yellow lines in Figure 10a). This indicates that the excursion into the western basin is essential to yield a stronger water mass transformation.

The temperature and salinity distribution of the particles released in the realistic simulation also show that the water mass transformation of AW depends on the pathway the water takes through the basin; particles that cross the Mohn Ridge toward the west are colder and fresher when they leave the model domain than the particles that stay within the front current (Figures 10b and 10c). The cooling and freshening of the water mass that crosses the mid-ocean ridge by frontal instabilities is likely due to mixing with the cold and fresh water masses within the Greenland Basin. Furthermore, the excursion across the ridge increases the transit time (not shown). Therefore, the cooling of the water mass continues as long as the water mass is exposed to the atmosphere.

5. Conclusions and Discussion

In this paper, we have investigated whether the flow along the Mohn Ridge and the flow along the Knipovich Ridge are connected in a Lagrangian sense. As the number of surface drifters and ARGO floats near the mid-ocean ridges is limited, we have additionally analyzed trajectories of numerical particles in a realistic and an idealized numerical simulation. These simulations allowed us not only to investigate the connection between the slope and front currents of the Norwegian Atlantic Current (NwAFC and NwASC, respectively) but also to trace water mass transformations along different pathways.

Based on this study, it is clear that care should be taken when using velocity and travel direction from surface drifters to derive circulation maps. These maps, as, for example, derived by Orvik and Niiler (2002), show the Eulerian mean velocity field but cannot provide any information on the connection between different branches in a Lagrangian sense. Based on the observed trajectories, we found only a weak connection between the northward flow along the Mohn Ridge and along the Knipovich Ridge, unlike how the NwAFC is normally schematized. Only 5 of the 40 surface drifters showed the traditional pathway north along both ridges. Instead, most drifters displayed exchange with the slope current (Figure 5a).

Trajectories in the realistic numerical simulations indicated a stronger connection between the flow along the Mohn Ridge and the Knipovich Ridge than the observed trajectories. However, the model results showed a clear branching of the flow along the Mohn Ridge into different paths to the north (Figure 6). Therefore, in the realistic numerical simulation, the front current along the Mohn Ridge did not form a one-to-one connection with the front current along the Knipovich Ridge either, corroborating the conclusions drawn from the observed trajectories.

Frequent exchange between the slope and front current was seen in the observed trajectories and the realistic model (Figures 2, 5 and 6). Many surface drifters and ARGO floats traveled along the 2,500 m isobath near 72°N toward the east (west) to join the slope (front) current on their path northward. This path was present in the realistic numerical simulation as well. Further north, floats crossed from the eastern branch of the West Spitsbergen Current to the western branch of the West Spitsbergen Current (or vice versa). The front current and slope current are therefore not isolated but clearly connected in a Lagrangian sense. Rossby, Prater, et al. (2009) observed a similar connection between the front current and the slope current just north of the Iceland-Scotland Ridge using RAFOS floats. Our results suggest that also north of 72°N significant exchange between the two branches occurs.

There are various mechanisms that can contribute to exchanges between the front and slope currents. The surface drifters in the Nordic Seas flow within the Ekman layer and are therefore subject to Ekman transport (Brambilla & Talley, 2006). Although the wind stress curl in the Nordic Seas is predominantly positive, wind reversals can occasionally enhance exchange between the boundary and the interior of the Lofoten Basin

and therefore enable crossovers between the slope and the front current. In addition to wind effects, the strong eddy variability near the Lofoten Islands provides a means for AW to enter the Lofoten Basin interior as well (Fer et al., 2020). The latter mechanism seems to be responsible for AW transport from the slope current to the interior at depth, whereas wind processes seem to steer the surface waters across the Vøring Plateau entering the Lofoten Basin from the south (Dugstad, Fer, et al., 2019).

Although wind effects are likely to play a role for the pathways of the surface drifters, the trajectories of the ARGO floats and the modeled trajectories from the realistic and idealized simulations are positioned below the Ekman layer. Below the surface, the mean circulation patterns are strongly dominated by topography (e.g., Nøst & Isachsen, 2003; Voet et al., 2010). Voet et al. (2010) observed the tight flow alignment with topography using so-called topostrophy derived from ARGO float trajectories, which is a measure of the flow alignment with isobaths. However, the region north of the Lofoten Basin is characterized by low values of topostrophy (his Figure 9), indicating that the ARGO float trajectories cross isobaths there. This is in agreement with our findings, where in addition to the ARGO floats, also, surface drifters showed similar behavior in this area. Such a crossover region could indicate that in this area the strength of eddies and meanders is of similar magnitude as along-flow mean velocities (Bower, 1991; Rossby, Prater, et al., 2009).

The numerous exchanges between the front current and the slope current lengthen the residence time of AW within the eastern basins of the Nordic Seas, which could enhance the total heat loss over the basin. Furthermore, the link between these two branches weakens the direct propagation of AW anomalies from the Greenland-Scotland Ridge to Fram Strait. It is therefore important to increase our knowledge not only on processes within the Lofoten Basin but also on the region north of 74°N and in particular on the local front current dynamics.

Analyses of trajectories in both the realistic and the idealized numerical configurations showed that AW transformation in the Nordic Seas depends on the path that the AW takes. Additionally, the water mass transformation itself could to some extent determine which path the AW will follow downstream. Our results suggest that the coldest and freshest water masses are formed along the front current, due to the frontal current instability and exchange with the western basin. Although not investigated in this study, the observed pathways are likely to display seasonal variations (e.g., Bosse & Fer, 2019). On longer time scales, it is known that the strength of the front current depends on the phase of the North Atlantic Oscillation (NAO); the front is weaker during the negative phase of the NAO (Raj et al., 2019). Also, under future scenarios, the front is expected to weaken, due to a reduction in the density gradient between the Lofoten Basin and the Greenland Basin (Ypma et al., 2020). If, due to the decrease in baroclinic instability, the exchange between the east and west reduces, the AW heat loss in the eastern basins could decrease and convection in the Greenland Basin could weaken due to a smaller supply of salty waters from the east.

Although not observed previously (Latarius & Quadfasel, 2016; Poulain et al., 1996; Rossby, Prater, et al., 2009), we found 28 ARGO floats and surface drifters that crossed the mid-ocean ridges. This might seem like a small number, but compared to the total number of observed trajectories that reached the mid-ocean ridges (90 floats), the observed cross-ridge exchange may be substantial. As in situ measurements suggest strong northward flow along the mid-ocean ridge (Bosse & Fer, 2019), it is surprising that out of the 564 surface drifters and 283 ARGO floats in the Nordic Seas, so few are found close to the Mohn and Knipovich Ridges. We would therefore encourage deployment of drifters within the strong northward flow along the mid-ocean ridge, to gain further insight in the pathways and residence time of AW in the eastern Nordic Seas.

Data Availability Statement

The ARGO data were collected and made freely available by the International Argo Program and the national programs that contribute to it (http://www.argo.ucsd.edu, http://argo.jcommops.org). The Argo Program is part of the Global Ocean Observing System. The ROMS simulation was performed on resources provided by UNINETT Sigma2-The National Infrastructure for High Performance Computing and Data Storage in Norway; the drifter simulations were performed on servers provided by the Norwegian Meteorological Institute in Oslo, Norway. The ROMS model fields are developed by Nils H. Kristensen and Martha Trodahl and are available at the Thredds Service at the Norwegian Meteorologial Institute (https://thredds.met.no/). The 3-D Langrangian simulations are developed with help from Knut-Frode

Dagestad and will be archived, open-access, at the Norstore research data archive (https://archive.norstore.no/). The idealized model fields and corresponding Lagrangian simulation are archived, open-access, online (at https://doi.org/10.4121/uuid:6c686dea-0079-4040-ac8b-3680e62c5ed5).

Acknowledgments

We would like to thank two anonymous reviewers whose comments improved this paper. S. L. Ypma and S. Georgiou were supported by NWO (Netherlands Organization for Scientific Research) VIDI Grant 86413011 awarded to C. A. Katsman. J. S. Dugstad received funding from the Research Council of Norway, through the project *Water mass transformation processes and vortex dynamics in the Lofoten Basin in the Norwegian Sea (ProVoLo)*, Project 250784. The surface drifters used in this study are obtained from the Global Drifter Programme (https://www.aoml.noaa.gov/phod/gdp/). This study has been conducted using E.U. Copernicus Marine Services Information. The altimeter products were produced by Ssalto/Duacs and distributed by Aviso +, with support from CNES (https://www.aviso.altimetry.fr). The authors would like to thank Nils Brüggemann for his help and input in developing the idealized model simulation and Carine van der Boog for providing assistance to download the ARGO data.

References

Bosse, A., & Fer, I. (2019). Mean structure and seasonality of the Norwegian Atlantic Front Current along the Mohn Ridge from repeated glider transects. *Geophysical Research Letters*, *46*, 13,170–13,179. https://doi.org/10.1029/2019GL084723

Bosse, A., Fer, I., Søiland, H., & Rossby, T. (2018). Atlantic water transformation along its poleward pathway across the Nordic Seas. *Journal of Geophysical Research: Oceans*, *123*, 6428–6448. https://doi.org/10.1029/2018JC014147

Bower, A. S. (1991). A simple kinematic mechanism for mixing fluid parcels across a meandering jet. *Journal of Physical Oceanography*, *21*(1), 173–180.

Bower, A. S., Lozier, S., Biastoch, A., Drouin, K., Foukal, N., Furey, H., et al. (2019). Lagrangian views of the pathways of the Atlantic Meridional Overturning Circulation. *Journal of Geophysical Research: Oceans*, *124*, 5313–5335. https://doi.org/10.1029/2019JC015014

Brakstad, A., Våge, K., Håvik, L., & Moore, G. W. K. (2019). Water mass transformation in the Greenland Sea during the period 1986–2016. *Journal of Physical Oceanography*, *49*(1), 121–140.

Brambilla, E., & Talley, L. D. (2006). Surface drifter exchange between the North Atlantic subtropical and subpolar gyres. *Journal of Geophysical Research*, *111*, C07026. https://doi.org/10.1029/2005JC003146

Budéus, G., & Ronski, S. (2009). An integral view of the hydrographic development in the Greenland Sea over a decade. *The Open Oceanography Journal*, *3*, 8–39.

Chafik, L., & Rossby, T. (2019). Volume, heat, and freshwater divergences in the subpolar North Atlantic suggest the Nordic Seas as key to the state of the Meridional Overturning Circulation. *Geophysical Research Letters*, *46*, 4799–4808. https://doi.org/10.1029/2019GL082110

Dagestad, K.-F., Röhrs, J., Breivik, O., & Ådlandsvik, B. (2018). Opendrift v1. 0: A generic framework for trajectory modelling. *Geoscientific Model Development*, *11*(4), 1405–1420.

Dugstad, J., Fer, I., LaCasce, J., Sanchez de La Lama, M., & Trodahl, M. (2019). Lateral heat transport in the Lofoten Basin: Near-surface pathways and subsurface exchange. *Journal of Geophysical Research: Oceans*, *124*, 2992–3006. https://doi.org/10.1029/2018JC014774

Dugstad, J. S., Koszalka, I., Isachsen, P. E., Dagestad, K.-F., & Fer, I. (2019). Vertical structure and seasonal variability of the inflow to the Lofoten Basin inferred from high resolution Lagrangian simulations. *Journal of Geophysical Research: Oceans*, *124*, 9384–9403. https://doi.org/10.1029/2019JC015474

Eldevik, T., Nilsen, J. E. O., Iovino, D., Olsson, K. A., Sandø, A. B., & Drange, H. (2009). Observed sources and variability of Nordic Seas overflow. *Nature Geoscience*, *2*(6), 406.

Fer, I., Bosse, A., & Dugstad, J. (2020). Norwegian Atlantic Slope Current along the Lofoten Escarpment. *Ocean Science*, *16*(3), 685–701.

Hansen, B., & Østerhus, S. (2000). North Atlantic-Nordic Seas exchanges. *Progress in oceanography*, *45*(2), 109–208.

Isachsen, P. E. (2015). Baroclinic instability and the mesoscale eddy field around the Lofoten Basin. *Journal of Geophysical Research: Oceans*, *120*, 2884–2903. https://doi.org/10.1002/2014JC010448

Koszalka, I., LaCasce, J. H., Andersson, M., Orvik, K. A., & Mauritzen, C. (2011). Surface circulation in the Nordic Seas from clustered drifters. *Deep Sea Research Part I: Oceanographic Research Papers*, *58*(4), 468–485.

Koszalka, I., LaCasce, J. H., & Mauritzen, C. (2013). In pursuit of anomalies—Analyzing the poleward transport of Atlantic Water with surface drifters. *Deep Sea Research Part II: Topical Studies in Oceanography*, *85*, 96–108.

Latarius, K., & Quadfasel, D. (2016). Water mass transformation in the deep basins of the Nordic Seas: Analyses of heat and freshwater budgets. *Deep Sea Research Part I: Oceanographic Research Papers*, *114*, 23–42.

Lozier, M. S., Li, F., Bacon, S., Bahr, F., Bower, A. S., Cunningham, S. A., et al. (2019). A sea change in our view of overturning in the subpolar North Atlantic. *Science*, *363*(6426), 516–521.

Lumpkin, R., & Pazos, M. (2007). Measuring surface currents with surface velocity program drifters: The instrument, its data, and some recent results. *Lagrangian analysis and prediction of coastal and ocean dynamics* (Vol. 2, pp. 39). Cambridge University Press Cambridge.

Marshall, J., Adcroft, A., Hill, C., Perelman, L., & Heisey, C. (1997). A finite-volume, incompressible Navier Stokes model for studies of the ocean on parallel computers. *Journal of Geophysical Research*, *102*(C3), 5753–5766.

Mauritzen, C. (1996). Production of dense overflow waters feeding the North Atlantic across the Greenland-Scotland Ridge. Part 1: Evidence for a revised circulation scheme. *Deep Sea Research Part I: Oceanographic Research Papers*, *43*(6), 769–806.

Messias, M.-J., Watson, A. J., Johannessen, T., Oliver, K. I. C., Olsson, K. A., Fogelqvist, E., et al. (2008). The Greenland Sea tracer experiment 1996–2002: Horizontal mixing and transport of Greenland Sea intermediate water. *Progress in Oceanography*, *78*(1), 85–105.

Nøst, O. A., & Isachsen, P. E. (2003). The large-scale time-mean ocean circulation in the Nordic Seas and Arctic Ocean estimated from simplified dynamics. *Journal of Marine Research*, *61*(2), 175–210.

Olsson, K. A., Jeansson, E., Anderson, L. G., Hansen, B., Eldevik, T., Kristiansen, R., et al. (2005). Intermediate water from the Greenland Sea in the Faroe Bank Channel: Spreading of released sulphur hexafluoride. *Deep Sea Research Part I: Oceanographic Research Papers*, *52*(2), 279–294.

Orvik, K. A., & Niiler, P. (2002). Major pathways of Atlantic water in the northern North Atlantic and Nordic Seas toward Arctic. *Geophysical Research Letters*, *29*(19), 1896. https://doi.org/10.1029/2002GL015002

Paris, C. B., Helgers, J., Van Sebille, E., & Srinivasan, A. (2013). Connectivity modeling system: A probabilistic modeling tool for the multi-scale tracking of biotic and abiotic variability in the ocean. *Environmental Modelling & Software*, *42*, 47–54.

Poulain, P.-M., Warn-Varnas, A., & Niiler, P. P. (1996). Near-surface circulation of the Nordic Seas as measured by Lagrangian drifters. *Journal of Geophysical Research*, *101*(C8), 18,237–18,258.

Raj, R. P., Chatterjee, S., Bertino, L., Turiel, A., & Portabella, M. (2019). The Arctic front and its variability in the norwegian sea. *Ocean Science*, *15*(6), 1729–1744.

Rossby, T., Ozhigin, V., Ivshin, V., & Bacon, S. (2009). An isopycnal view of the Nordic Seas hydrography with focus on properties of the Lofoten Basin. *Deep Sea Research Part I: Oceanographic Research Papers*, *56*(11), 1955–1971.

Rossby, T., Prater, M. D., & Søiland, H. (2009). Pathways of inflow and dispersion of warm waters in the Nordic Seas. *Journal of Geophysical Research*, *114*, C04011. https://doi.org/10.1029/2008JC005073

Ruan, X., & Callies, J. (2019). Mixing-driven mean flows and submesoscale eddies over mid-ocean ridge flanks and fracture zone canyons. *Journal of Physical Oceanography*, *50*, 175–195.

Saloranta, T. M., & Svendsen, H. (2001). Across the Arctic front west of Spitsbergen: High-resolution CTD sections from 1998–2000. *Polar Research*, *20*(2), 177–184.

Segtnan, O. H., Furevik, T., & Jenkins, A. D. (2011). Heat and freshwater budgets of the Nordic seas computed from atmospheric reanalysis and ocean observations. *Journal of Geophysical Research*, *116*, C11003. https://doi.org/10.1029/2011JC006939

Smith, W. H. F., & Sandwell, D. T. (1997). Global sea floor topography from satellite altimetry and ship depth soundings. *Science*, *277*(5334), 1956–1962.

Spall, M. A. (2010). Non-local topographic influences on deep convection: An idealized model for the Nordic Seas. *Ocean Modelling*, *32*(1–2), 72–85.

Spall, M. A. (2011). On the role of eddies and surface forcing in the heat transport and overturning circulation in marginal seas. *Journal of Climate*, *24*(18), 4844–4858.

Trodahl, M., & Isachsen, P. E. (2018). Topographic influence on baroclinic instability and the mesoscale eddy field in the northern North Atlantic Ocean and the Nordic Seas. *Journal of Physical Oceanography*, *48*(11), 2593–2607.

van Aken, H. M., Budeus, G., & Hähnel, M. (1995). The anatomy of the Arctic frontal zone in the Greenland Sea. *Journal of Geophysical Research*, *100*(C8), 15,999–16,014.

van Sebille, E., Griffies, S. M., Abernathey, R., Adams, T. P., Berloff, P., Biastoch, A., et al. (2018). Lagrangian ocean analysis: Fundamentals and practices. *Ocean Modelling*, *121*, 49–75.

Voet, G., Quadfasel, D., Mork, K. A., & Søiland, H. (2010). The mid-depth circulation of the Nordic Seas derived from profiling float observations. *Tellus A: Dynamic Meteorology and Oceanography*, *62*(4), 516–529.

Walczowski, W. (2013). Frontal structures in the West Spitsbergen Current margins. *Ocean Science*, *9*(6), 957–975.

Ypma, S. L., Spall, M. A., Lambert, E., Georgiou, S., Pietrzak, J. D., & Katsman, C. A. (2020). The contrasting dynamics of the buoyancy-forced Lofoten and Greenland Basins. *Journal of Physical Oceanography*, *50*(5), 1227–1244.